Dislocation processes in the deformation of nanocrystalline aluminium by molecular-dynamics simulation

VESSELIN YAMAKOV[1], DIETER WOLF[1]*, SIMON R. PHILLPOT[1], AMIYA K. MUKHERJEE[2] AND HERBERT GLEITER[3]

[1]Argonne National Laboratory, 9700 S. Cass Avenue, Argonne, Illinois 60439, USA
[2]University of California, Davis, California 95616, USA
[3]Forschungszentrum Karlsruhe, Institut für Nanotechnologie, Karlsruhe, 76021 Germany
*e-mail: wolf@anl.gov

Published online: 1 September 2002; doi:10.1038/nmat700

The mechanical behaviour of nanocrystalline materials (that is, polycrystals with a grain size of less than 100 nm) remains controversial. Although it is commonly accepted that the intrinsic deformation behaviour of these materials arises from the interplay between dislocation and grain-boundary processes, little is known about the specific deformation mechanisms. Here we use large-scale molecular-dynamics simulations to elucidate this intricate interplay during room-temperature plastic deformation of model nanocrystalline Al microstructures. We demonstrate that, in contrast to coarse-grained Al, mechanical twinning may play an important role in the deformation behaviour of nanocrystalline Al. Our results illustrate that this type of simulation has now advanced to a level where it provides a powerful new tool for elucidating and quantifying—in a degree of detail not possible experimentally—the atomic-level mechanisms controlling the complex dislocation and grain-boundary processes in heavily deformed materials with a submicrometre grain size.

The unusual mechanical behaviour of nanocrystalline materials[1], showing either greatly enhanced ductility[2–4] or dramatically increased strength and hardness[5–7] is thought to arise from the intricate interplay between dislocation and grain-boundary processes (see, for example, ref. 8). The common low-temperature plastic-deformation mechanism in coarse-grained metals and ceramics involves the continuous nucleation of dislocations from Frank-Read sources and their glide, on well-defined slip systems, through the crystal. In a polycrystalline material, the size of these sources cannot exceed the grain size. Because the stress needed for their operation is inversely proportional to the size of the source, this deformation mechanism can operate only down to a grain size of typically about 1 μm. For a smaller grain size, mobile dislocations must be nucleated from other sources, such as the grain boundaries (GBs) or grain junctions.

Using a recently developed, massively parallel molecular-dynamics (MD) code for the simulation of polycrystal plasticity[9], here we demonstrate for the case of nanocrystalline Al the complex interplay of various dislocation and GB processes responsible for the low-temperature deformation behaviour of materials with submicrometre grain size. A unique aspect of our work, arising from our ability to deform to rather large plastic strains and to consider a relatively large grain size, is the observation of deformation under very high GB and dislocation densities. We are thus able to identify the intra- and intergranular dislocation and GB processes in a deformation regime where they compete on an equal footing, and to gain atomic-level insights into the underlying mechanisms not currently possible experimentally. These insights include the observation of mechanical twinning in a nanocrystalline material and the formation of a new grain during the deformation. Our simulations thus illustrate the manner in which dislocation-based deformation of nanocrystalline materials differs qualitatively from the well-studied behaviour of coarse-grained materials.

All our simulations involve idealized columnar, <110>-textured microstructures, consisting of four grains of identical size and regular-hexagonal shape. The grain orientations were chosen such that all 12 GBs in the simulation cell are asymmetric high-angle <110> tilt boundaries. The carefully selected <110> column axis ensures that, following their

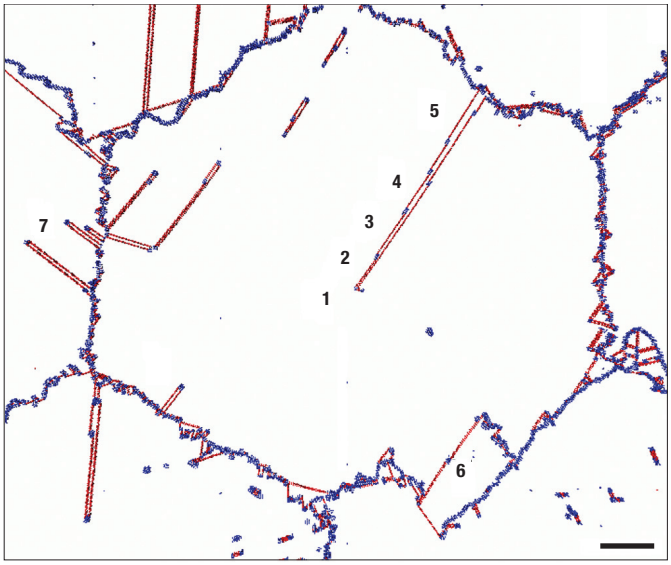

1. A B C A B C A B C A B C A B C A B C A B C
2. A B C A B A B C A B C A B C A B C A B C
3. A B C A B A C A B C A B C A B C A B C
4. A B C A B A C B C A B C A B C A B C
5. A B C A B A C B C B C A B C A B C

Figure 1 Snapshot for a grain diameter of 70 nm at 10.3% plastic strain, revealing two well-known mechanisms for the formation of two distinct types of deformation twins (seen in processes 1–5 and 6, respectively). The process labelled 7 involves the nucleation of double-Shockley partials, leaving behind extrinsic stacking faults. Red dots denote atoms in an h.c.p. environment. Blue dots denote atoms that are 'defected', that is, neither in an f.c.c. nor h.c.p. environment, including atoms with broken nearest-neighbour bonds. The stacking sequences for regions 1–5 are shown below the figure and described in the text. Scale bar, 10 nm.

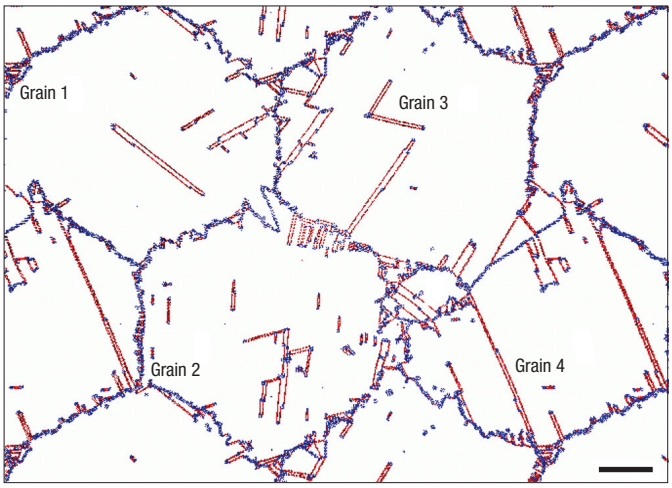

Figure 2 Snapshot at 11.9% plastic strain for a grain diameter of 45 nm. A variety of processes involving dislocation–dislocation and dislocation–GB interactions has now taken place. (A movie of the full simulation appears in the Supplementary Information). Red and blue dots as described in Fig. 1. Scale bar, 10 nm.

nucleation, dislocations can glide in each grain on either of two (111) slip systems, unimpeded by the three-dimensionally periodic border conditions imposed on the simulation cell. In principle, such textured two-dimensional (2D) microstructures are found in nature in the form of columnar thin films, although these films are usually attached to a substrate, whereas our microstructures are free-standing thin films consisting of infinitely long cylindrical grains. This idealized simulation geometry clearly imposes certain constraints (see below) on the dislocation processes that can thus occur. However, it enables us to probe a considerably larger grain-size regime than ever studied before in fully three-dimensional (3D) microstructures, thus providing a fuller picture of the interplay between dislocation and GB processes during the deformation (see Methods and ref. 9.).

We used a many-body interatomic potential for Al fitted, along with other parameters, to the elastic constants[10]. The potential has been slightly modified for a higher degree of smoothness at the cut-off radius[9]. Although it leaves other physical parameters practically unchanged, this modification increases the stacking-fault energy from 104 to 122 mJ m^{-2}, that is, closer to the experimental values[11] ranging between 120 and 142 mJ m^{-2}.

Our recent study of textured Al polycrystals using this approach revealed the onset of plastic flow when the applied tensile stress exceeded the threshold stress for the nucleation of extended dislocations from the GBs or grain junctions[9]. Below this critical stress (of about 2.3 GPa, corresponding to a resolved shear stress on the slip planes of about 1 GPa), the system deformed very slowly via a GB-based mechanism rendering the network of straight, sharp GBs almost unchanged during the deformation. These simulations also revealed the detailed mechanism for the nucleation of extended dislocations from the GBs, involving the successive emission of both the leading and trailing Shockley partial dislocations (partials) connected by a stacking fault. Following their complete nucleation, these dislocations travel across the grains on one of the available (111) slip planes, until they are destroyed in another GB. Also, as the grain size decreases down to about 20 nm, the nucleation of complete dislocations is no longer possible, and the dislocation-slip mechanism ceases to be operational[9], in favour of a GB-based deformation mechanism[12–14].

Here we focus on deformation processes in nanocrystalline Al in a regime where dislocation and GB processes compete with each other on an equal footing; this requires considerably larger strains, and hence involves much higher dislocation densities than in any earlier study. Under these conditions, in a coarse-grained material, deformation twinning represents a powerful elementary deformation process, provided the material has a low stacking-fault energy, for example, Cu. As is consistent with the well-known mechanism[15] described in the literature on coarse-grained materials with low stacking-fault energy, Fig. 1 reveals deformation twinning by the successive emission of partial dislocations from the same GB on adjacent (111) planes. The ABCABC stacking sequences of the three types of (111) planes in the face-centred cubic (f.c.c.) lattice, labelled A, B and C, in five regions of the twinned grain are indicated in the schematic at the bottom of the figure. Letters in red, denoting those having the same neighbours on both sides, indicate planes in a local hexagonal close-packed (h.c.p.) ABAB (or ACAC or BCBC) stacking sequence. The five regions are: (1) perfect f.c.c. crystal; (2) intrinsic stacking fault; (3) extrinsic stacking fault; (4) two twin boundaries separated by two (111) planes; and (5) more widely separated twins. Common neighbour analysis[16] was used to identify perfect crystal atoms as being either in an h.c.p. (red atoms in Fig. 1) or f.c.c. environment (not shown).

The observation of deformation twinning in a nanocrystalline material is very surprising[17], not only because of the very small grain size but also because Al has a high stacking-fault energy although, on the basis of structural analysis[18], there are suggestions of its existence in materials with a low stacking-fault energy, such as Cu. Previous simulations for Cu revealed the emission of extrinsic stacking faults from the GBs during the early stages of the deformation[13]. However, their coordinated nucleation and propagation across the grain interiors, giving rise to deformation twinning during the later stages of the deformation, has so far eluded detection because of the small grain size to which these simulations were necessarily limited.

Our simulations also reveal a second, entirely different, mechanism for twin formation (labelled 6 in Fig. 1). This mechanism, previously described by Gleiter[19] in the context of coarse-grained materials, involves the splitting and subsequent migration of a GB segment, leaving behind two coherent twin boundaries. In addition, process 7 in Fig. 1 reveals the mechanism observed earlier[13] for the emission of extrinsic stacking faults (see also process 3 in Fig. 1) from the GBs via the nucleation of double-Shockley partials[15,20]. By contrast with the nucleation of single partial dislocations, this process is known to require extremely large local stresses.

As the plastic strain increases, the dislocation concentration in the grain interiors continues to increase, giving rise to various types of intragranular dislocation–dislocation interaction processes associated with the glide of extended dislocations on different slip systems. Most of these processes are well known from extensive deformation studies in single crystals and coarse-grained polycrystals[21–23]. Among the best known is the formation of Lomer–Cottrell locks[15,23], seen inside grains 2 and 3 in Fig. 2. These locks, formed by two stacking faults meeting at an angle of 70.5° and connected by a stair -rod dislocation[21] (blue dots), are identified by the crossing double red lines. The dynamics of Lomer–Cottrell lock formation are revealed in the Supplementary Information movie.

In addition to the above intragranular processes, our simulations also reveal a variety of unanticipated intergranular processes (described in detail in the following two paragraphs), involving the interaction of dislocations with GBs and deformation twins. Their net combined effect after 11.9% plastic strain is shown in Fig. 2 for a grain diameter of 45 nm.

The considerable roughness of the initially flat GBs is particularly noticeable in Fig. 2 (see also Fig. 1). This roughness arises entirely from dislocation–GB interaction processes, as shown by the fact that, for a stress slightly below the dislocation–nucleation threshold, the GBs remain perfectly straight during the entire deformation simulation. Moreover, a new grain labelled A has been nucleated at those GBs that were especially active during these emission/absorption/twin-formation events. In addition, Fig. 2 reveals a mechanism for what, at first sight, appears to be GB splitting (see the GB between grains 2 and 3). However, detailed analysis reveals that the ordered deformation substructure in grain 2 arises from the same mechanism of double-Shockley-partial emission trailed by extrinsic stacking faults seen in Fig. 1 (process 7). We note that the cores of the double-Shockley partials are aligned, presumably owing to elastic interactions; this eventually leads to the formation of a new dislocation boundary.

The sequence of snapshots in Fig. 3 captures in detail the underlying GB and dislocation processes involved in the formation of the new grain, A, shown in Fig. 2. The nucleation of the new grain starts by the emission of a complete 1/2[110] dislocation from the GB between grains 3 and 4 (process 1 in Fig. 3a). The complex core structure labelled 1' was formed by two such dislocations, emitted, however, onto different slip planes. As seen in Fig. 3b, this new, almost immobile complex core structure subsequently begins to continuously emit partials, producing a growing twin lamella by "partial-dislocation breakaway"[21] (process 2). This lamella grows further by absorbing additional 1/2[110] dislocations emitted from the same GB (process 1 in Fig. 3b), leading to its increased size in Fig. 3c. The development of the new grain also involves the emission of another twin lamella (labelled 3 in Fig. 3c) together with extrinsic stacking faults terminated by double-Shockley partials (labelled 4; see also process 7 in Fig. 1). Finally, the rather complex deformation substructure thus formed subsequently coalesces to form the final grain A in Fig. 3d and Fig. 2.

There are inherent limitations in the observed deformation behaviour arising from the columnar simulation geometry chosen here. Although it enables us to probe the deformation behaviour in a considerably larger grain-size regime than has been previously studied[12–14], this geometry means that the microstructure is effectively 2D, consisting of infinitely long cylindrical grains. This in itself is not an entirely unphysical situation, given that such columnar 2D microstructures are commonly observed in thin films, although they are usually attached to a substrate. However, such a columnar geometry limits the dislocations emitted from the GBs to be parallel to each other and to the GBs; moreover, owing to the rather short periodic repeat length of the simulation cell in the <110> texture direction (for details, see Methods and ref. 9), these dislocations are always straight, that is, free of kinks.

In a columnar thin film with a <110> texture axis, only four of the 12 slip systems present in a 3D grain structure can be activated during the deformation. Each columnar grain therefore contains only two active slip planes[9] rather than the four in a 3D grain microstructure. In practice, two independent slip systems are sufficient to accommodate any deformation in the x–y plane; however, usually only one of these (known as the primary slip system) is active during plastic deformation. Also, suppression of kinks on the dislocation lines will suppress certain types of dislocation dynamics and modify the dislocation–nucleation process from the GBs, giving rise to some hardening of the material and an increase in the dislocation–nucleation stress, as shown by the extremely high threshold stress of 2.3 GPa observed for this simulation geometry[9]. In spite of these limitations, as critical test cases, our simulations correctly reproduce key elementary dislocation processes, such as the structure of dissociated dislocations in f.c.c. metals, Lomer–Cottrell lock formation and the mechanism for mechanical twinning.

In coarse-grained Al, the propensity for deformation twinning observed in Figs 1–3 would be very surprising, given that Al has a rather high stacking-fault energy. However, it is also known that the relationship between the stacking-fault energy and the occurrence of deformation twinning is rather indirect and, in fact, is entirely unexplored in nanocrystalline materials[17]. Our observations strongly suggest that a re-examination of the basic models for twinning, with particular emphasis on nanocrystalline grain size, may be timely.

Our simulations mostly cover new ground, as yet experimentally unexplored, not only as far as the small grain size is concerned but also in other important aspects. By contrast with typical *in situ* transmission electron microscopy experiments, the insights gained from Figs 1–3 inherently capture bulk deformation behaviour, unencumbered by any mechanical stresses and surface effects that inadvertently affect the observations in thin-film specimens. Also, even for coarse-grained

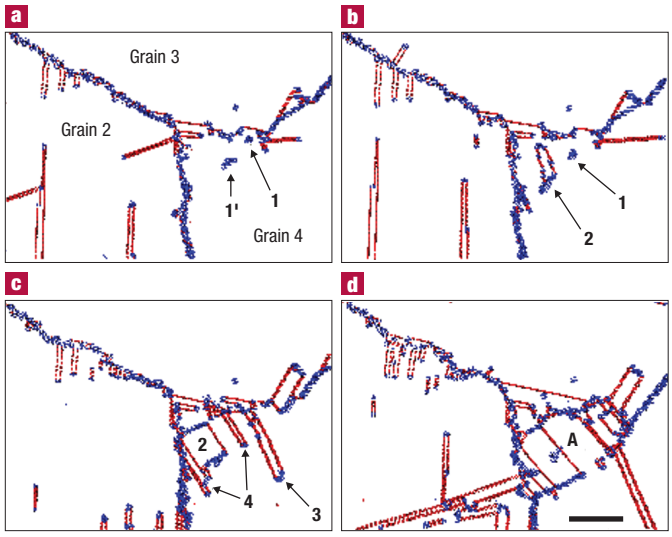

Figure 3 Successive snapshots of the vicinity of the triple junction connecting grains 2, 3 and 4, demonstrating the mechanism by which the new grain A in Fig. 2 was formed. a, Plastic strain ε = 6.09%; **b**, 6.19%; **c**, 6.76%; and **d**, 8.71%. Four distinct processes labelled 1–4 are revealed; these are described in the text. Red and blue dots as described in Fig. 1. Scale bar, 10 nm.

materials, it would be extremely difficult to extract the underlying deformation mechanisms from experiments in the type of dynamical and atomistic detail available from Figs 1–3.

The above simulations of well-characterized, although highly idealized, model systems illustrate the opportunities offered by large-scale MD simulations towards unravelling the complex interplay between dislocation and GB processes in nanocrystalline materials. However, it is equally important to be aware of the fundamental limitations inherent to this approach. Apart from being limited to relatively small model systems (even in the columnar geometry considered here), by their very nature MD simulations are restricted to very high stresses and, hence, strain rates. For example, a strain of 1% occurring in 10 ns of simulation time corresponds to a strain rate of 10^6 s^{-1}. It is therefore imperative that, for each type of simulation, the characteristic stresses and timescales associated with the deformation-rate-limiting dynamical processes be compared with all other relevant characteristic stresses and timescales in the system.

In the present simulations, in spite of the large tensile stresses (of 2.3 GPa) and strain rates (~10^7 s^{-1}) under which deformation was observed, typical dislocation-glide velocities (of about 500 m s^{-1}) are well below the sound velocity (of about 3,664 m s^{-1} in the [100] direction for this potential[10], compared to the experimental value of 3,050 m s^{-1}). More importantly, however, the resolved shear stresses, of the order of 1 GPa on the (111) slip planes of our system, are well below the theoretical shear strength, σ_{th}, for Al. Frenkel's perfect-crystal shear model gives an estimate of $\sigma_{th} = G/2\pi$; with G = 32.5 GPa for Al at 0 K (to which our potential was fitted[10]), we obtain a value of σ_{th} = 5.18 GPa at 0 K, and slightly lower at room temperature. This value is in good agreement with recent nanoindentation experiments on Al thin films, which yielded values of σ_{th} in the range of 4.2–4.5 GPa (refs 24, 25), demonstrating that the Frenkel formula is well satisfied for Al.

The high strain rates in MD simulations were recently also examined in high-temperature deformation simulations of nanocrystalline Pd[26]. These simulations revealed that, in spite of the extremely high strain rates (of >10^7 s^{-1}), the Coble-creep equation[27] describing GB diffusion creep in coarse-grained materials was quantitatively reproduced. Most importantly, the activation energy for the creep rate was found to agree completely with that obtained from separate simulations of self-diffusion in bicrystalline GBs, that is, in the absence of applied stress[28]. These simulations demonstrate that the artificially high strain rates present in MD simulations, and the necessarily high applied stresses, need not in any way affect the underlying GB physics.

We think it will soon be possible to elucidate the physical mechanisms controlling technologically important processes, such as superplastic forming. The ability to completely characterize the highly inhomogeneous state of internal stress should also lead to the development of better materials-physics-based deformation models.

METHODS

Our simulations involve idealized, <110>-textured microstructures, consisting of four grains of identical size and regular-hexagonal shape; the grains are oriented relative to the tensile axis (horizontal, x axis) of the simulation cell by rotations about [110] by angles 0°, 30°, 60° and 90°. The 12 high-angle GBs in the system therefore consist of three groups of identical asymmetric [110] tilt GBs: whereas the 30° and 90° boundaries are high-energy GBs, with a highly disordered atomic structure[28–30], the 60° tilt GBs have a dislocation structure because their misorientation is vicinal to the coherent-twin 70.53° tilt misorientation. The <110> column axis (z direction) ensures that, following their nucleation, dislocations can glide on either of two {111} slip systems in each grain, unimpeded by the 3D-periodic border conditions imposed on the simulation cell.

The minimum thickness of the simulation cell in the columnar (z) direction is determined by the cut-off radius of the interatomic potential used for the simulations. Our simulation cell thus contains only ten periodically repeated (110) planes; their interplanar spacing of $(2/4a_0)^{1/2}$ results in an initial z thickness of ~$3.5a_0$ (or ~1.42 nm for a_0 = 4.03 Å for our embedded-atom-method potential for Al (ref. 10). By contrast with the z direction, the simulation-cell size in the x–y plane is determined solely by the grain size; for values ranging between 20 and 70 nm, our simulated systems thus contain between 97,000 and 1,021,000 atoms.

All our MD simulations were carried out under constant tensile loads of 2.3–2.5 Pa and at a temperature of T = 300 K (the melting point for this interatomic potential was estimated[10] at 940 K, compared to the experimental value of 933 K). The Parrinello–Rahman constant-stress technique[31] combined with the Nose–Hoover thermostat[32] and an integration time step of 0.5 × 10^{-15} s was used to achieve the constant stress–constant temperature dynamics of the system. For further details, see ref.9.

Received 19 March 2002; Accepted 24 May 2002.

References

1. Koch, C. C. & Suryanarayana, C. in *Microstructure and Properties of Materials* Vol. 2 (ed. Li, J. C. M.) Ch. 6 380–385 (World Scientific, Singapore, 2000).
2. Karch, J., Birringer, R. & Gleiter, H. Ceramics ductile at low-temperature. *Nature* **330,** 556–558 (1987).
3. McFadden, S. X., Mishra, R. S., Valiev, R. Z., Zhilyaev, A. P. & Mukherjee, A. K. Low-temperature superplasticity in nanostructured nickel and metal alloys. *Nature* **398,** 684–686 (1999).
4. Kim, B. N., Hiraga, K., Morita, K. & Sakka, Y. A high-strain-rate superplastic ceramic. *Nature* **413,** 288–291 (2001).
5. Siegel, R. W. Mechanical properties of nanophase materials. *Mater. Sci. Forum* **235–238,** 851–860 (1997).
6. Morris, D. G. & Morris, M. A. Hardness, strength, ductility and toughness of nanocrystalline materials. *Mater. Sci. Forum* **235–238,** 861–872 (1997).
7. Nesladek, P. & Veprek, S. Superhard nanocrystalline composites with hardness of diamond. *Phys. Status Solidi A* **177,** 53–62 (2000).
8. Yip, S. Nanocrystals—the strongest size. *Nature* **391,** 532–533 (1998).
9. Yamakov, V., Wolf, D., Salazar, M., Phillpot, S. R. & Gleiter, H. Length-scale effects in the nucleation of extended lattice dislocations in nanocrystalline Al by molecular-dynamics simulation. *Acta Mater.* **49,** 2713–2722 (2001).
10. Ercolessi, F. & Adams, J. B. Interatomic potentials from 1st-principle calculations – the force-matching method. *Europhys. Lett.* **26,** 583–588 (1994).
11. Noonan, J. R. & Davis, H. L. Truncation-induced multilayer relaxation of the Al(110) surface. *Phys. Rev. B* **29,** 4349–4355 (1984).
12. Schiotz, J., DiTolla, F. D. & Jacobsen, K. W. Softening of nanocrystalline metals at very small grain sizes. *Nature* **391,** 561–563 (1998).
13. Schiotz, J., Vegge, T., DiTolla, F. D. & Jacobsen, K. W. Atomic-scale simulations of the mechanical deformation of nanocrystalline metals. *Phys. Rev. B* **60,** 11971–11983 (1999).
14. Swygenhoven, H. V., Spaczer, M., Caro, A. & Farkas, D. Competing plastic deformation mechanisms in nanophase metals. *Phys. Rev. B* **60,** 22–25 (1999).
15. Weertman, J. & Weertman, J. R. *Elementary Dislocation Theory* (Oxford Univ. Press, New York, 1992).
16. Jonsson, H. & Andersen, H. C. Icosahedral ordering in the Lennard-Jones liquid and glass. *Phys. Rev. Lett.* **60,** 2295 –2298 (1988).
17. El-Danaf, E., Kalindi, S. R. & Doherty, R. Influence of grain size and stacking-fault energy on deformation twinning. *Metall. Mater. Trans. A* **30,** 1223–1233 (1999).
18. Ungar, T., Ott, S., Sanders, P. G., Borbely, A. & Weertman, J. R. Dislocations, grain size and planar faults in nanostructured copper determined by high resolution X-ray diffraction and a new procedure of peak profile analysis. *Acta Mater.* **46,** 3693–3699 (1998).
19. Gleiter, H. in *Progress in Materials Science,* Chalmers Anniversary Volume (eds Christian, J. W., Haasen, P. & Massalski, T. B.) 172 (Pergamon, Oxford, 1981).
20. Hirth, J. P. & Hoagland, R. G. Extrinsically dissociated dislocations in simulated aluminium. *Phil. Mag. A* **78,** 529–532 (1998).
21. Hirth, J. P. & Lothe, J. *Theory of Dislocations* Ch. 10-3 (Wiley, New York, 1992).
22. Zhou, S. J., Preston, D. L., Lomdahl, P. S. & Beazley, D. M. Large-scale molecular dynamics simulations of dislocation intersection in copper. *Science* **279,** 1525–1527 (1998).
23. Bulatov, V., Abraham, F. F., Kubin, L., Devincre, B. & Yip, S. Connecting atomistic and mesoscale simulations of crystal plasticity. *Nature* **391,** 669–672 (1998).
24. Gouldstone, A., Koh, H.-J., Zeng, K.-Y., Giannakopoulos, A. E. & Suresh, S. Discrete and continuous deformation during nanoindentation of thin films. *Acta Mater.* **48,** 2277–2295 (2000).
25. Gouldstone, A., Van Vliet, K. J. & Suresh, S. Simulation of defect nucleation in a crystal. *Nature* **411,** 656 (2001).
26. Yamakov, V., Wolf, D., Phillpot S. R. & Gleiter, H. Grain-boundary diffusion creep in nanocrystalline palladium by molecular-dynamics simulation. *Acta Mater.* **50,** 61–73 (2002).
27. Coble, R. L. A model for boundary-diffusion controlled creep in polycrystalline materials. *J. Appl. Phys.* **34,** 1679–1682 (1963).
28. Keblinski, P., Phillpot, S. R., Wolf, D. & Gleiter, H. Self-diffusion in high-angle fcc-metal grain boundaries by molecular-dynamics simulation. *Phil. Mag. A* **79,** 2735–2761 (1999).
29. Keblinski, P., Phillpot, S. R., Wolf, D. & Gleiter, H. Thermodynamic criterion for the stability of amorphous intergranular films in covalent materials. *Phys. Rev. Lett.* **77,** 2965–2968 (1996).
30. Wolf, D. in *The Encyclopedia of Materials: Science and Technology* (ed. Cahn, R.) 3597–3609 (Elsevier, Amsterdam, 2001).
31. Parrinello, M. & Rahman, A. Polymorphic transitions in single crystals: A new molecular dynamics method. *J. Appl. Phys.* **52,** 7182–7190 (1981).
32. Melchionna, S., Ciccotti, G. & Holian, B. L. Hoover NPT dynamics for systems varying in shape and size. *Mol. Phys.* **78,** 533–544 (1993).

Acknowledgements

V.Y., D.W. and S.R.P. are supported by the US Department of Energy, Basic Energy Sciences-Materials Science under contract W-31-109-Eng-38. V.Y. also thanks the DOE/BES Computational Materials Science Network (CMSN) for support. A.K.M. acknowledges support from the National Science Foundation-Division of Materials Research. We are grateful for computer time on the Cray-T3E at the John-von-Neumann Institut for Computing in Jülich, Germany, and on the Chiba City Linux cluster at Argonne National Laboratory.

Correspondence and requests for materials should be addressed to D.W.

Supplementary information is available on the Nature Materials website (http://www.nature.com/nmat)

Competing financial interests

The authors declare that they have no competing financial interests.

A movie of the full simulation of deformation of nanocrystalline Al with grains of 45 nm in diameter shows nucleation of dislocations from the grain boundaries at the initial stages of deformation and deformation twinning at later stages. Formation of a new grain out of a triple junction is seen after 140 ps deformation time (as indicated in the lower-right corner in the movie). Common-neighbor analysis was used to identify perfect-crystal atoms as being either in a local hcp (red atoms) or fcc environment (atoms not shown). Blue atoms are 'defected', i.e., neither in an fcc nor hcp environment, including atoms with broken nearest-neighbor bonds. The hcp atoms indicate twin boundaries as single red lines or stacking faults as double red lines. The isolated blue dots of 'defected' atoms represent dislocation cores.